

Investigating the influence of grain-size distribution and its uncertainty on ash dispersal modelling

Mattia de' MICHELII VITTURI^(a) Augusto NERI^(a) Federica PARDINI^(a) Maria Vittoria SALVETTI^(b) Antonio SPANU^(c)

1. Motivation and objective

Volcanic ash clouds represent a major hazard for populations living nearby volcanic centers producing a risk for humans and a potential threat to crops, ground infrastructures, and aviation traffic.

Such a phenomenon is affected by numerous uncertainty sources since its dynamics is largely affected by initial and boundary conditions that cannot be predicted in advance.

In this presentation we present the main outcomes of a modelling study aimed to investigate the variation, together with its uncertainty, of the mixture grain-size distribution during the dispersal process.

2. Mt. Etna Case Study

The analysis presented in this work has been performed for dispersal conditions referred to the event of November 24, 2006 at Mt. Etna. Plume height was about 4.3 km above sea level¹. For this event the volcanic cloud showed horizontal stripes oriented perpendicularly to the prevailing wind direction (as observed at other volcanoes, eg. Klyuchevskaya in Kamchatka and Eyjafjallajökull in Iceland). Through field and satellite data it was possible to closely observe the dispersal process. It has been hypothesized that the stripes are produced by Kelvin-Helmholtz instabilities associated to the presence of the volcanic ash itself.

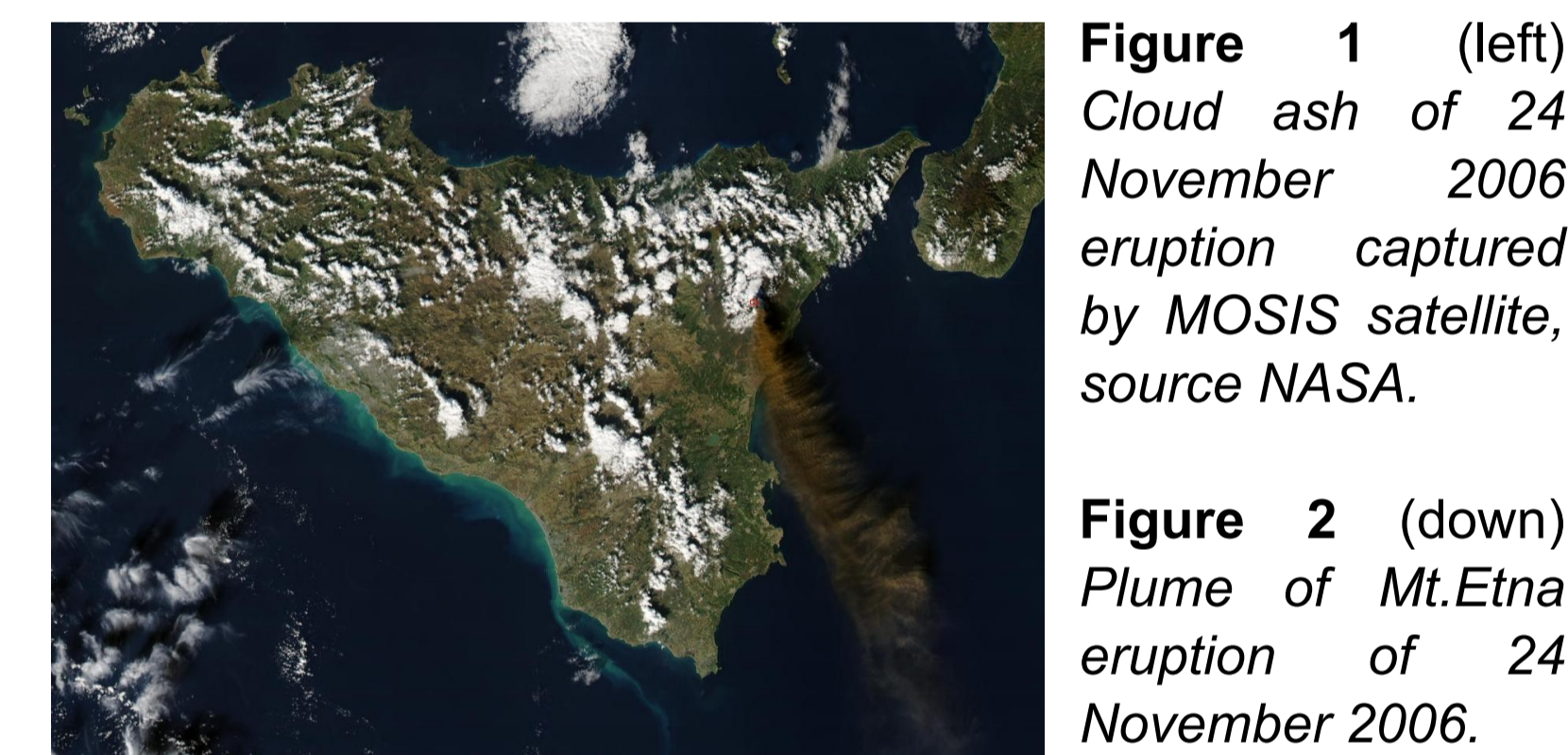


Figure 1 (left) Cloud ash of 24 November 2006 eruption captured by MOSIS satellite, source NASA.

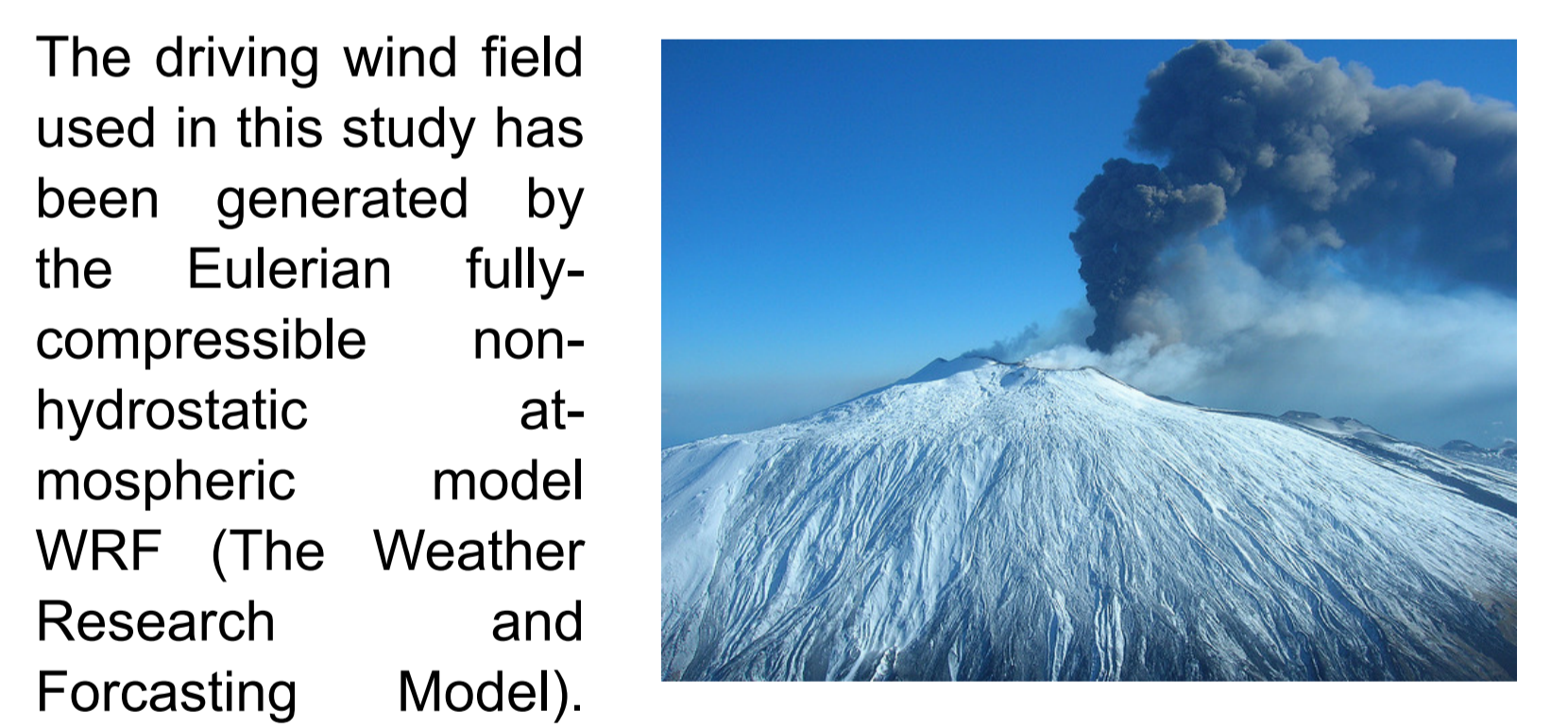


Figure 2 (down) Plume of Mt. Etna eruption of 24 November 2006.

The driving wind field used in this study has been generated by the Eulerian fully-compressible non-hydrostatic atmospheric model WRF (The Weather Research and Forecasting Model). Because the wind direction was nearly constant during the event after 12:00PM, we have investigated the phenomenon using high-resolution two-dimensional simulations. The wind field generated for this simulation covers a domain of about 40 km horizontally and 6 km vertically and Kelvin-Helmholtz instabilities are present in the output in the vertical range between 3300m and 4300m⁽²⁾ one hour after the beginning of the simulation.

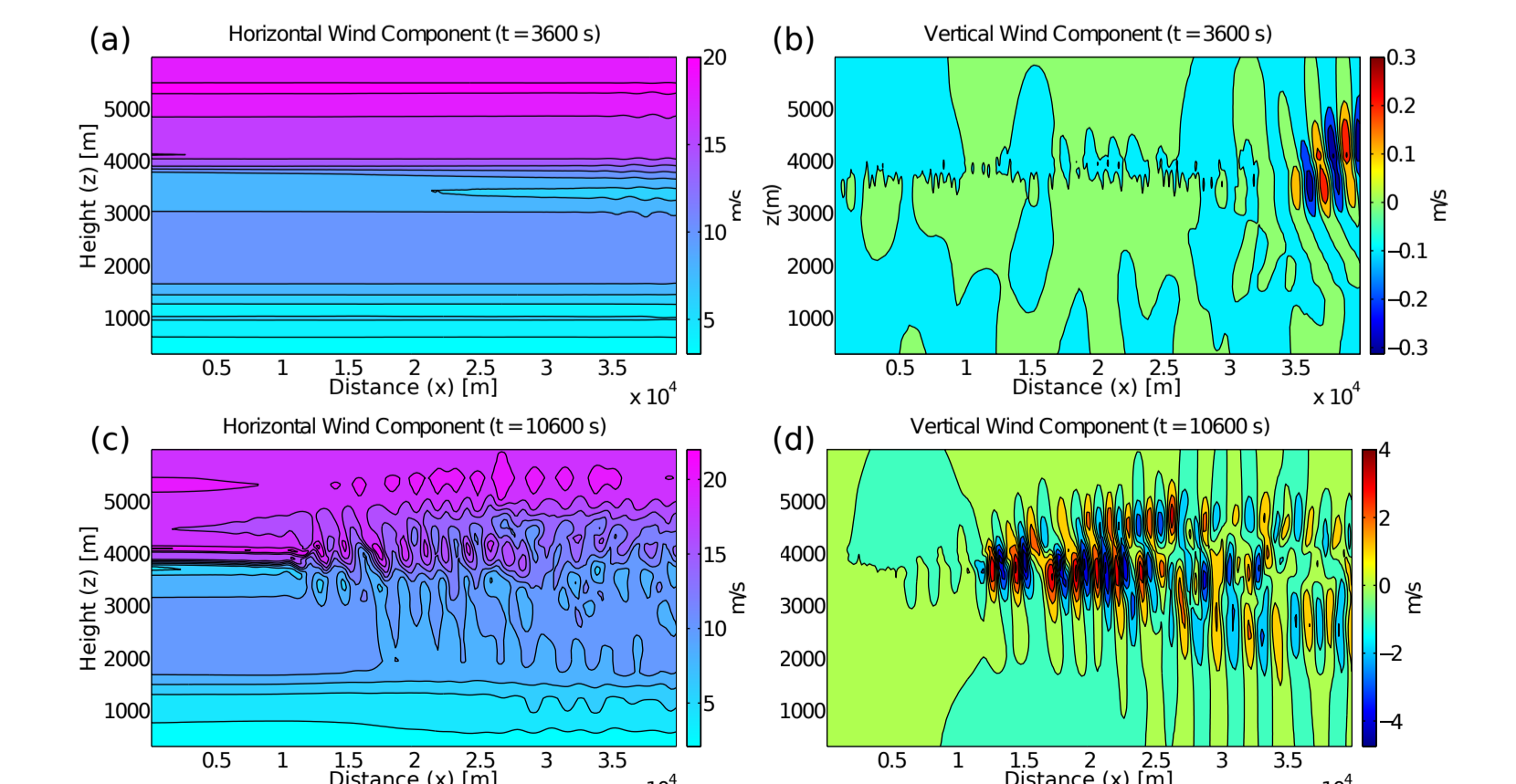


Figure 3. Background flow field computed by using the 2D High-resolution mesoscale WRF. This model allowed to hypothesize the formation of Kelvin-Helmholtz instabilities as responsible for the generation of oscillations in the dispersal process².

3. The Lagrangian particle model LPAC

For this application we used a Lagrangian particle model, named LPAC³, to simulate the transport of ash under the action of the atmospheric field computed by the mesoscale model WRF. The equations of particle motion are derived expressing the Lagrangian acceleration as the sum of the forces acting along its trajectory. In order to increase the stability of the model, drag forces were calculated implicitly as a function of relative velocity, particle diameter and Reynolds number⁴. No turbulence and aggregation effects were considered. Due to the low concentration of ash in the atmosphere, a one-way coupling between the background flow field and the particles was assumed. In addition, in these simulations, each "particle", or parcel, is assumed representative of the same amount (mass) of pyroclastic material, and not of a single ash particle. To better investigate the distribution of the parcels during the process, the domain has been sub-divided into 4 vertical stripes and, in each stripe, a distinction between the particles in the atmosphere and on the ground has been made, resulting in 8 sub-domains (named Air 1-4 and Ground 1-4). Particles are released 2km downwind the left boundary of the domain, with a prescribed size distribution.

4. Grain Size Distribution

For volcanic ash particles, the size is generally described as mass fractions in the Krumbain logarithmic scale⁵, i.e.:

$$\varphi = -\log_2(d/d_0), \text{ with } d_0 = 1\text{mm.}$$

For this work, the uncertainty in the grain-size distribution has been described by assuming a range of values for the main parameters describing the ash particles: mean diameter μ and standard deviation σ of the grain size distribution and the sphericity ψ of the particles.

5. Lagrangian simulations results

Before carrying out the full uncertainty quantification analysis, it is interesting to look at the results of LPAC obtained for a particular set of the input parameters, and then varying only one of the input parameters at a time. In Figure 5 the results of a simulation with $\mu=1$, $\sigma=1.5$ and the sphericity $\psi=0.7$ are presented, with the different colors representing parcels of particles with different sizes (red for the smallest particles). In addition, in the bottom panels, the histograms of the size of the particles in the four stripes in the atmosphere (upper row) and on the ground (lower row) are plotted. In addition, in each panel the mean diameter and the standard deviation of the grain size distribution are reported. We can see how only the distribution in the portion of the domain closer to the release is representative of the original one.

In Figs. 6-8 the effects of varying only one parameter at a time on the grain size distributions after 3 hours of simulation are presented (when an almost steady-state is reached).

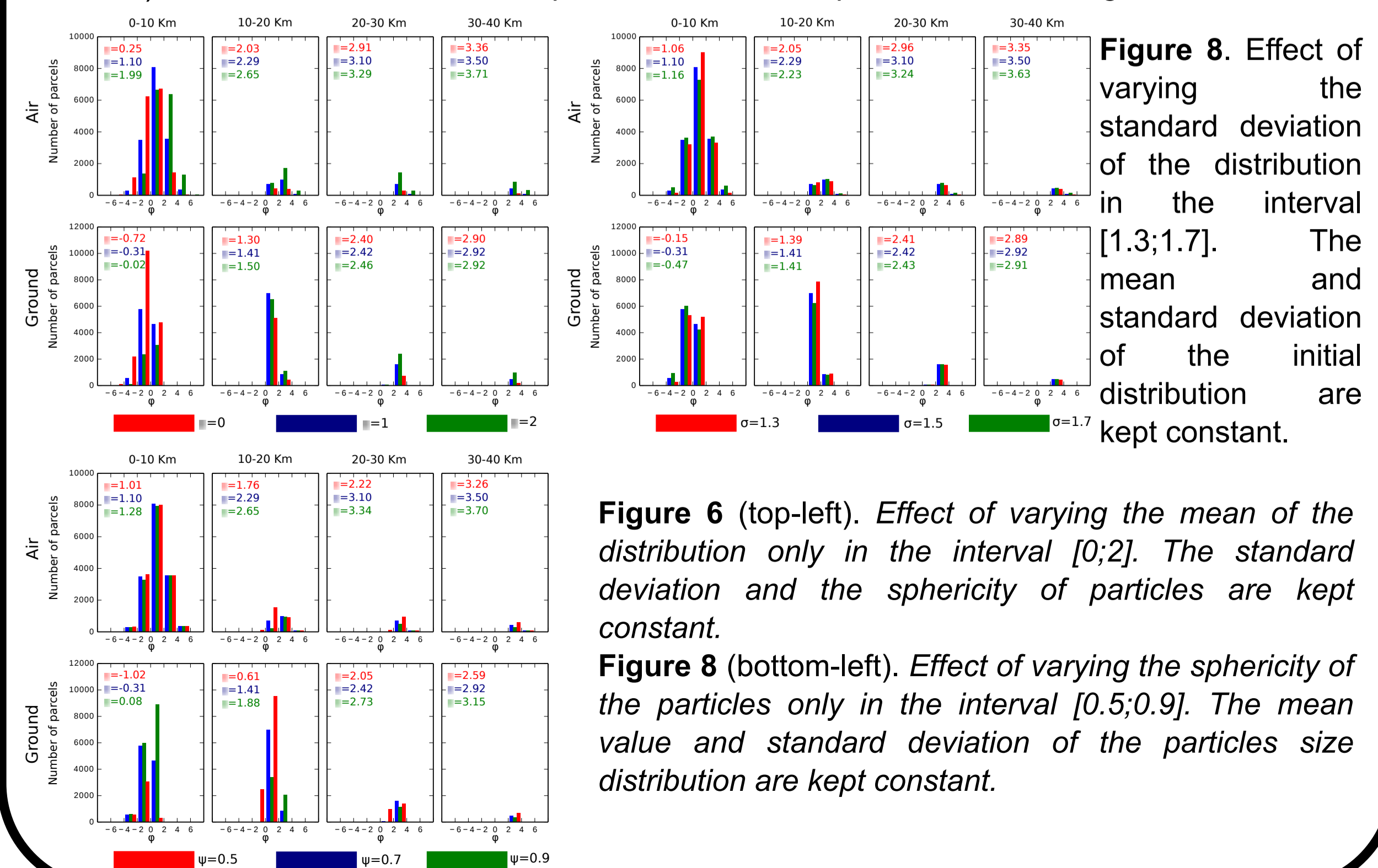


Figure 5. Lagrangian simulation of the particles dispersion in the atmosphere (top). The color is representative of the size of the particles. On the bottom the grain size distributions in four stripes of the domain are plotted for the particles in the atmosphere and on the ground.

[LINK TO THE VIDEO](#)

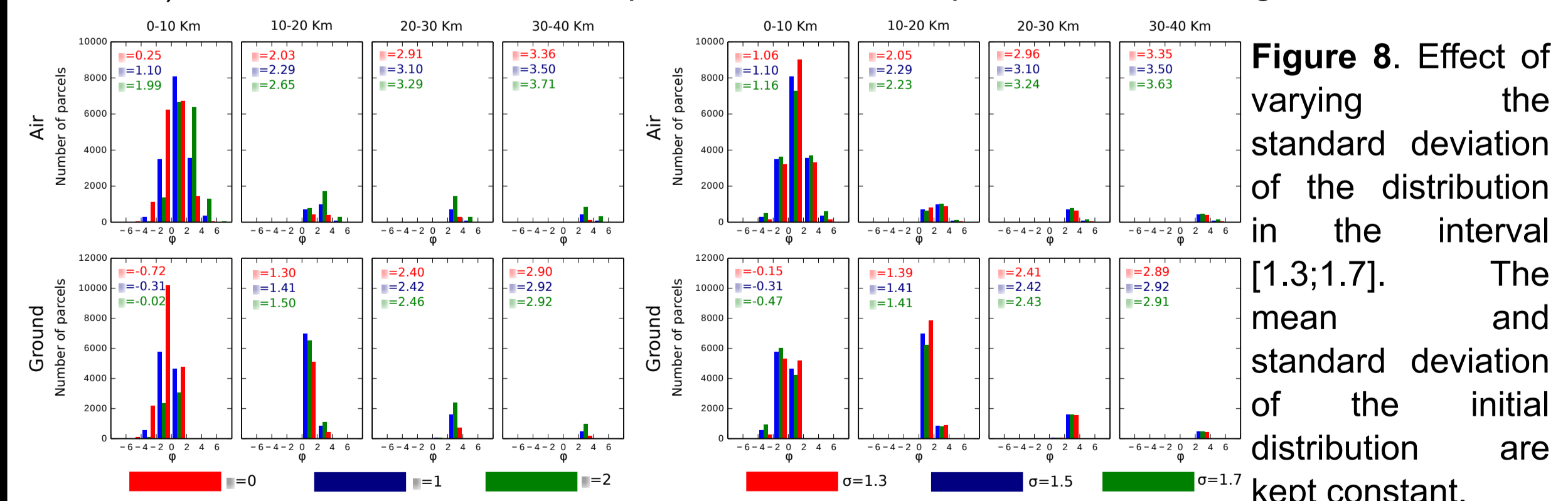


Figure 6. Effect of varying the mean of the distribution only in the interval [0,2]. The standard deviation and the sphericity of particles are kept constant.

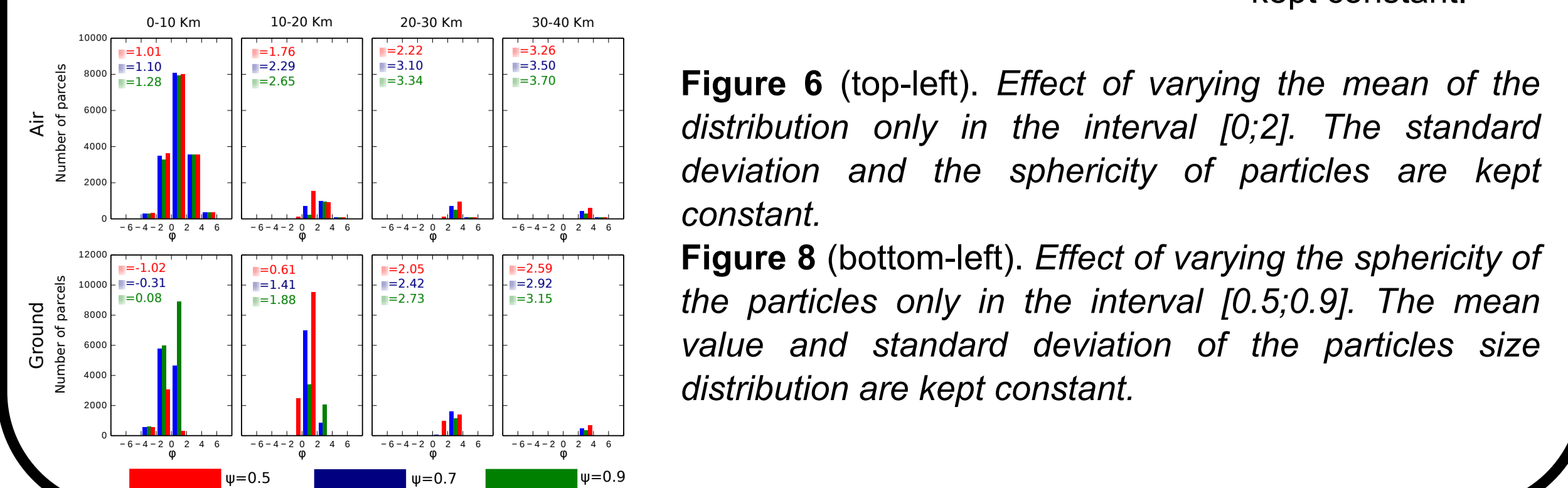
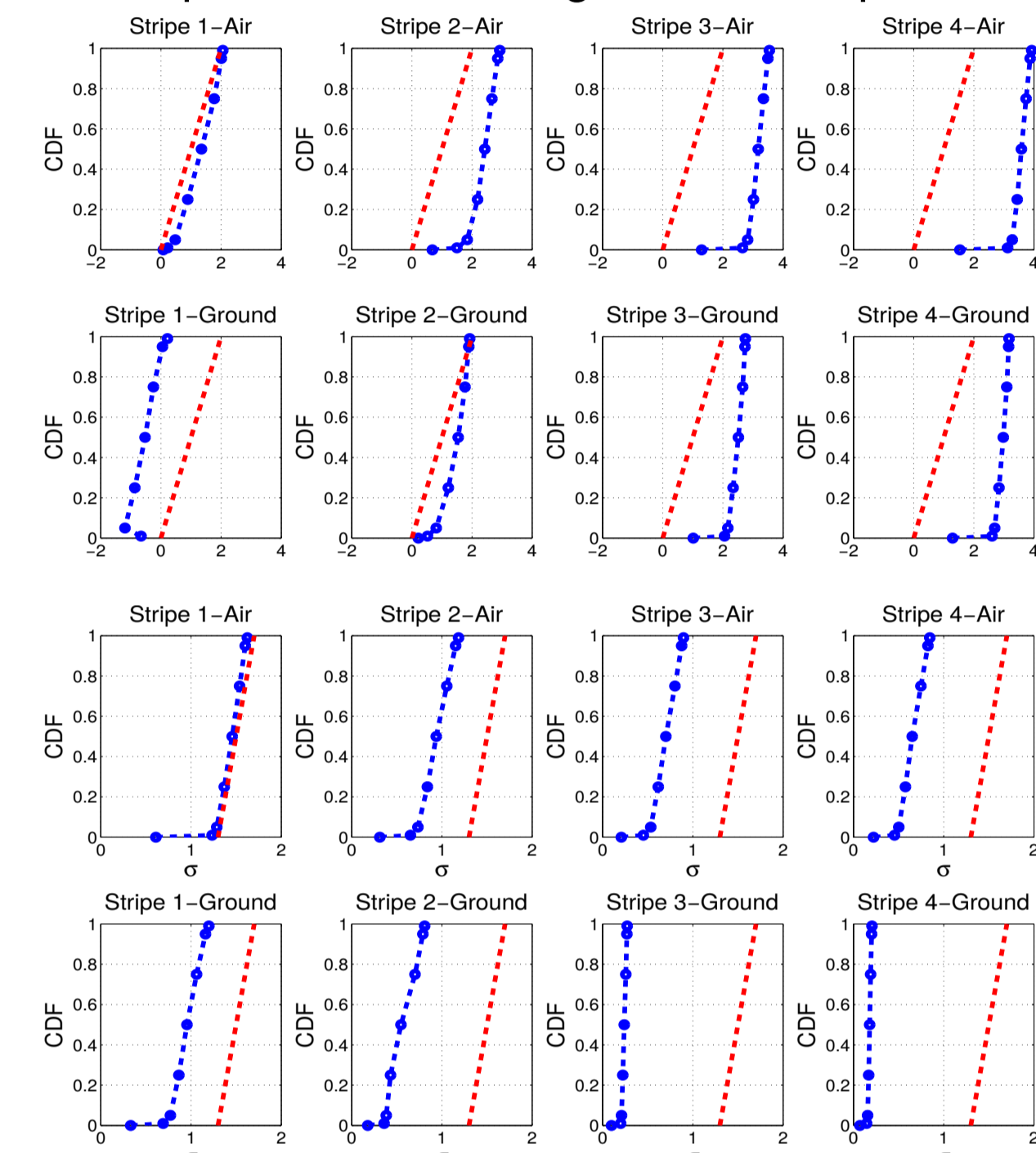


Figure 8. Effect of varying the sphericity of the particles only in the interval [0.5,0.9]. The mean value and standard deviation of the particles size distribution are kept constant.

6. Uncertainty quantification analysis

The DAKOTA toolkit from Sandia National Labs has been adopted to perform uncertainty quantification (UQ) and sensitivity analysis. In the present work we have chosen to adopt as UQ technique the so-called Generalized Polynomial Chaos Expansion, which is included within the class of Stochastic Expansion Method. The term "Chaos" simply refers to the uncertainty in the input, while the term "Polynomial" is used because propagation of uncertainties in the outputs is described by reconstructing the output of the model as polynomials. The first step is to model the input variables through appropriate probability distributions: here we assumed a uniform distribution of the uncertain input parameters (see Figure 4). The choice of these distributions affects the basis used for the polynomial reconstruction of the output of the model (response functions). In this case Legendre polynomials have been used as the basis for the expansion and an order 7 for the polynomials reconstructed has provided a good compromise between accuracy and computational cost. The coefficients of the elements of the basis have been computed through appropriate quadrature formulas, requiring 343 simulations and 1.5 hours on 46 CPUs. Once the expansion coefficients have been calculated, the polynomials have been used as emulators of the response functions and several statistics were evaluated numerically. In particular 10000 samples have been evaluated on the expansion to compute the cumulative distribution functions of the probabilities of the parameters describing the grain size distributions in the four stripes, in the atmosphere and on the ground. 7 cumulative probability levels (0.01, 0.05, 0.25, 0.5, 0.75, 0.95, 0.99) have been fixed and mapped into the corresponding response levels and the results are plotted in Figure 9. In addition, in Table 1 other statistical parameters related to the uncertainty in the grain size distributions in the atmosphere and on the ground are reported.



Response function t=10600s				
	Stripe 1 air	Stripe 2 air	Stripe 3 air	Stripe 4 air
Mean	1.12	2.27	3.08	3.51
Mode	0.89	2.42	3.17	3.58
Response function t=10600s				
	Stripe 1 ground	Stripe 2 ground	Stripe 3 ground	Stripe 4 ground
Mean	-0.39	1.33	2.41	2.90
Mode	-0.25	1.76	2.65	3.09
Response function t=10610800s number of parcels				
	Stripe 1 air	Stripe 2 air	Stripe 3 air	Stripe 4 air
Mean	1.41	0.89	0.66	0.61
Mode	1.45	0.83	0.61	0.57
Response function t=10610800s number of parcels				
	Stripe 1 ground	Stripe 2 ground	Stripe 3 ground	Stripe 4 ground
Mean	0.91	0.51	0.23	0.17
Mode	0.86	0.70	0.22	0.16
Response function t=10610800s number of parcels				
	Stripe 1 air	Stripe 2 air	Stripe 3 air	Stripe 4 air
Mean	3517	1843	907	593
Mode	3613	1554	380	229
Response function t=10610800s number of parcels				
	Stripe 1 ground	Stripe 2 ground	Stripe 3 ground	Stripe 4 ground
Mean	10693	7693	1689	525
Mode	8606	6831	1396	237

Figure 9 (left-top). Cumulative distribution functions of the mean of the grain size distributions computed in every stripe. The red curve of each plot represents the initial distribution of the released particles.

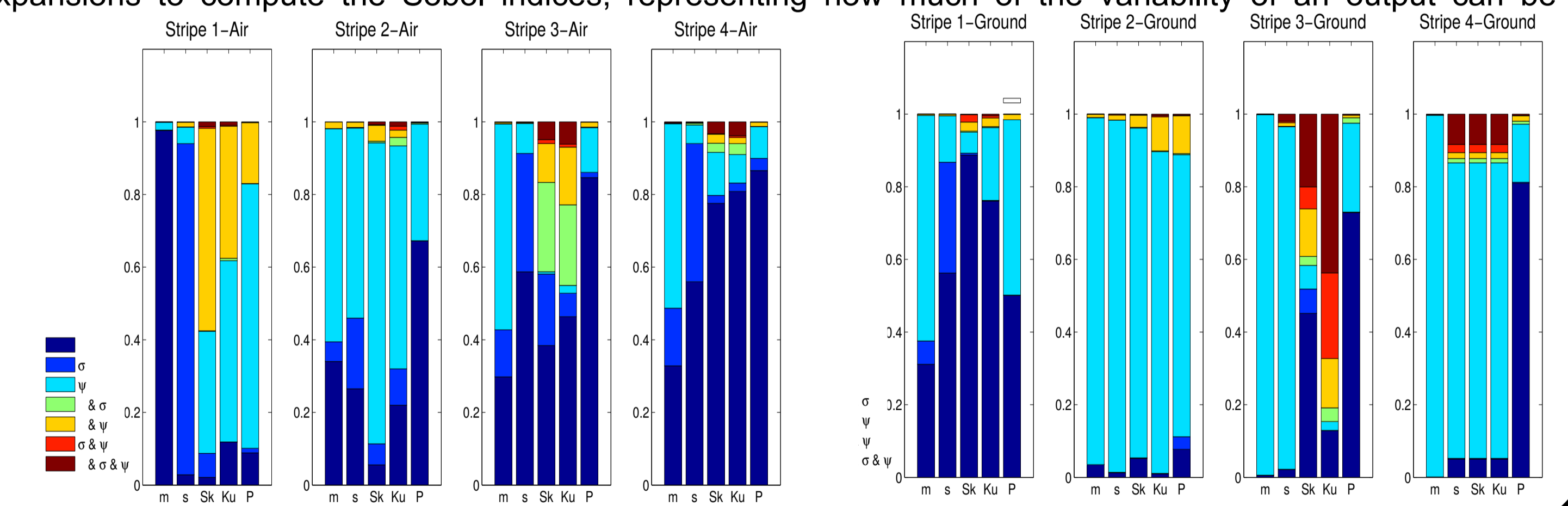
Figure 10 (left-bottom). Cumulative distribution functions of the standard deviation of the grain size distribution. The red curve of each plot represents the initial distribution of the released particles.

Table 1. Mean and the most probable values of μ and σ and number of parcels present in the four stripes (in air and on the ground) three hours after the beginning of the release in the atmosphere.

Figure 11. Sobol Indices for the parameters characterizing the grain size distribution of the particles in the four stripes in the air (left) and on the ground (right).

7. Sensitivity Analysis

A variance-based sensitivity analysis was also performed to quantify the global sensitivity indices of the response functions to the uncertain input parameters. 10,000 samples have been evaluated using the polynomial expansions to compute the Sobol indices, representing how much of the variability of an output can be apportioned to the variability prescribed to the input parameters. The sensitivity analysis shows that the variability of the sphericity of particles, controlling the drag and consequently the settling velocity of the particles, exerts a major role in determining the range of grain-size distribution parameters of the particles deposited on the ground in the four stripes, whereas the variability of the parameters of the grain-size distributions in the atmosphere are mainly controlled by variability of the mean value and sphericity of the initial distribution.



8. Conclusions

Based on the outcomes of the UQ and SA these are the main conclusions of the study:

- 1) ash dispersal process is able to effectively segregate particle of different sizes due to their different drag with the atmosphere. As a consequence, for a given plume height, the GSD of the mixture is mostly a function of distance from the emitting source, both airborne and on ground, independently from the original GSD;
- 2) for a given distance from source, GSDs (expressed as mean diameter and standard deviation) on ground and in air are not equal. Airborne GSD is significantly finer and less sorted with respect to that estimated on ground.
- 3) For a given distance from source, the GSD is mostly controlled by particle sphericity. Such control is stronger on ground than in air where also the mean diameter and sorting of the initial GSD play a significant role.
- 4) The uncertainty range in the mean diameter of the initial GSD of the mixture is significantly reduced with increasing distance from source. Such a reduction is more effective on ground than in air.
- 5) The uncertainty range on the standard deviation of the GSD of the mixture is almost constant with increasing distance from source in air, whereas it drastically reduces with distance on ground.

Acknowledgments. The work have been partially supported by the EU-funded project MEDSUV. Medsuv has received funding from the EU's Seventh Programme for research, technological development and demonstration under grant agreement No 308665.

References

- 1 D. Andronico, C. Spinetti, A. Cristaldi, and M.F. Buongiorno. Observations of Mt. Etna volcanic ash plumes in 2006: An integrated approach from ground-based and polar satellite NOAA-AVHRR monitoring system. Journal of volcanology and geothermal research, 180(2):135–147, 2009.
- 2 A. Spanu, S. Barsotti, M. De' Michieli Vitturi, M. Moustau, A. Mahalov, and A.B. Clarke. Kelvin-helmholtz instabilities in volcanic clouds and their effects on ash dispersal. In AGU Fall Meeting Abstracts, volume 1, page 2862, 2013.
- 3 M de' Michieli Vitturi, A Neri, T Esposti Ongaro, S Lo Savio, and E Boschi. Lagrangian modeling of large volcanic particles: Application to Vulcanian explosions. Journal of Geophysical Research: Solid Earth (1978–2012), 115(B8), 2010.
- 4 G. H. Ganser. A rational approach to drag prediction of spherical and nonspherical particles. Powder Technology, 77(2):143–152, 1993.
- 5 McManus. Grain size determination and interpretation. Techniques in sedimentology, 408, 1988.
- 6 B. M. Adams, W. E. Hart, M. S. Eldred, D. M. Dunlavy, P. D. Hough, A. A. Giunta, J. D. Griffin, M. L. Martinez-Canales, J. Watson, T. G. Kolda, et al. DAKOTA, a Multilevel Parallel Object-oriented Framework for Design Optimization, Parameter Estimation, Uncertainty Quantification, and Sensitivity Analysis: Version 4.0 Users Manual. United States. Department of Energy, 2006.